

Evidence for an Anti-charmed Baryon State *

CHR. RISLER

for the H1 collaboration

DESY, Notkestrasse 85, D-22607 Hamburg, Germany,
email: risler@mail.desy.de

We report on the observation of a narrow resonance in $D^{*-}p$ and $D^{*+}\bar{p}$ invariant mass combinations in deep-inelastic ep scattering at centre-of-mass energies of 300 and 320 GeV at HERA. The mass of the resonance is measured to be $3099 \pm 3(\text{stat.}) \pm 5(\text{syst.})$ MeV, the Gaussian width of $12 \pm 3(\text{stat.})$ MeV is compatible with the experimental resolution. The state can be interpreted as an anti-charmed baryon with minimal constituent quark composition $uudd\bar{c}$, together with the charge conjugate.

PACS numbers: 14.20.Lq, 14.80.-j

1. Introduction

In the last 2 years several experiments [1] have reported evidence of a narrow baryonic resonance with strangeness $S = +1$ in the invariant mass of K^+n combinations. These resonances can be interpreted as candidates for a strange pentaquark θ^+ , the minimal constituent quark content being $uudd\bar{s}$. These measurements were supported by similar observations [2] in the $K_S^0 p(\bar{p})$ spectrum, although this channel does not allow for the observation of exotic quantum numbers, since the K_S^0 is a linear combination of strangeness $S = +1$ and $S = -1$ states. However, there are also a number of high-energy experiments that do not confirm the observation of θ^+ candidates [3]. Also evidence for the pentaquark cascade states, Ξ_5^{--} and Ξ_5^0 with strangeness $S = -2$, has been reported [4]. The observations of possible θ^+ candidates have motivated H1 to search for a charmed pentaquark. The possible existence of such states had been discussed before [5]. The clearest charm signal is seen in the decay of the $D^{*\pm}$. Therefore a search

* Presented at the Cracow Ehipany Conference on Hadron Physics, Cracow, Poland, January 6-8, 2005

for resonances in the D^*p invariant mass spectrum was performed and evidence for a narrow baryonic resonance in the $D^{*-}p$ spectrum and its charge conjugate was found. In the following this analysis, which is published by the H1 collaboration [6], is briefly described.

2. Event Selection

The analysed data were collected with the H1 detector in the years 1996 to 2000 and correspond to an integrated luminosity of 75 pb^{-1} . A detailed description of the H1 detector can be found elsewhere [7]. Deep-inelastic scattering (DIS) events were selected by requiring a reconstructed scattered electron in the backward calorimeter of H1 and an exchanged photon virtuality of $Q^2 > 1 \text{ GeV}^2$. The kinematic range is further restricted to values of the inelasticity y of $0.05 < y < 0.7$ in order to ensure substantial hadronic final state energies in the central detector region. As an independent sample photoproduction (γp) events are used, where the scattered electron emits a quasireal photon and is not detected in the central detector but escapes in the beam pipe. Photoproduction events are selected by requiring $Q^2 < 1 \text{ GeV}^2$.

2.1. D^* and proton reconstruction

The decays of the charmed D^* mesons are reconstructed via the decay channel,

$$D^{*\pm} \rightarrow D^0 \pi_{sl}^\pm \rightarrow (K^\mp \pi^\pm) \pi_{sl}^\pm \quad ,$$

which provides a particularly clean D^* signal, although the branching ratios are low. A mass difference technique is applied, $\Delta M(D^*) = M(K\pi\pi) - M(K\pi)$, in order to improve the mass resolution. Candidates of three particle combinations are used if the reconstructed D^0 mass $M(K\pi)$ is close to its nominal value [8],

$$|M(K\pi) - M(D^0)_{PDG}| < 60 \text{ MeV} \quad .$$

After applying further cuts on the transverse momenta, $p_T(D^*) > 1.5 \text{ GeV}$ and $p_T(K) + p_T(\pi) > 2 \text{ GeV}$, the pseudorapidity $-1.5 < \eta(D^*) < 1.0$ and the production elasticity $z(D^*) = (E - p_z)_{D^*} / 2yE_e > 0.2$ of the D^* a good signal to background ratio in the $\Delta M(D^*)$ distribution is achieved, as shown in fig. 1a, yielding about 3500 D^* candidates. The background is mainly due to combinatorics, not involving any charm decays and can be estimated from the data by using the wrong charge D combinations, where instead of the oppositely charged K and π candidate tracks forming the D^0 , two tracks of the same charge are selected forming a doubly charged pseudo D

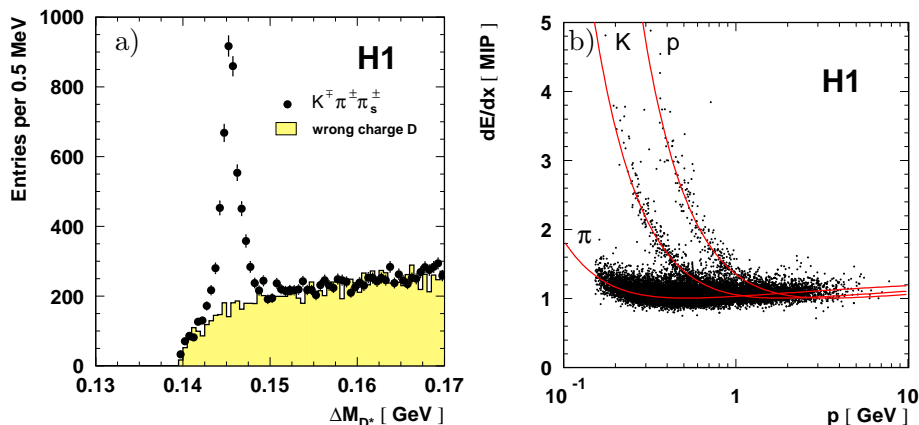


Fig. 1. (a) Distribution of the mass difference $\Delta M(D^*) = M(K\pi\pi) - M(K\pi)$ for DIS events ($Q^2 > 1 \text{ GeV}^2$). The background under the D^* signal is described by the wrong charge D combinations (see text). (b) Specific energy loss due to ionization dE/dx versus momentum for proton candidate tracks.

which further is combined with a slow pion track. The background under the D^* signal is well described by such wrong charge D combinations.

The D^* candidates are combined further with charged tracks originating from the primary vertex assigned the proton mass. These proton tracks are selected using the measurement of the ionisation loss dE/dx in the central drift chambers of H1. The average dE/dx resolution for minimal ionising particles is about 8% [9]. An example of the dE/dx distribution as a function of particle momenta is shown in fig. 1b. Bands for π , K and protons are clearly visible. The measurement is compared to the Bethe-Bloch-like parameterisation shown by the solid lines. From the difference of the measurement and the parameterisation the likelihood probabilities for different particle hypotheses are calculated which are used for particle identification.

3. D^*p signal

The selected D^* , fulfilling

$$|\Delta M(D^*) - (M(D^0)_{PDG} - M(D^*)_{PDG})| < 2.5 \text{ MeV} \quad ,$$

are further combined with the proton candidates. The invariant D^*p mass is formed again exploiting the mass difference method, $M(D^*p) = M(K\pi\pi p) -$

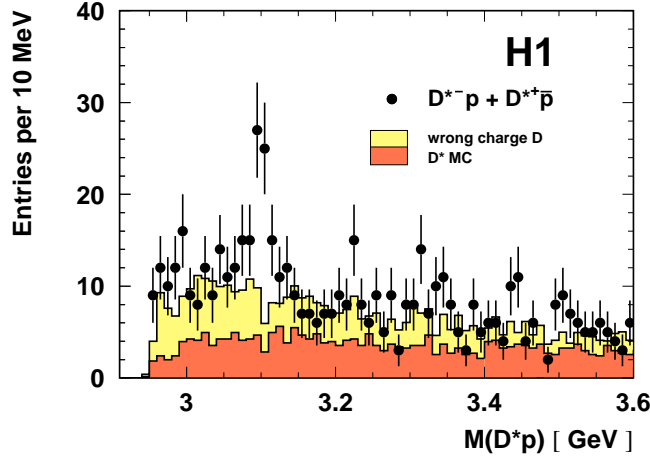


Fig. 2. Distribution in $M(D^*p)$ for opposite-charge D^*p combinations. The data are compared with the sum of a non-charm contribution estimated using the wrong charge D combinations and a simulated charm contribution (see text).

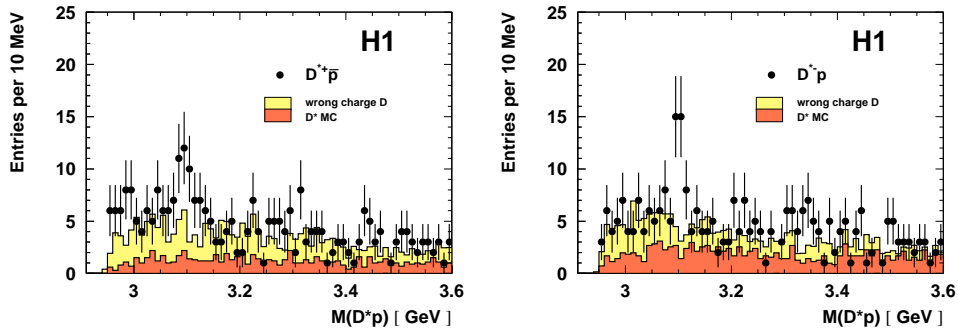


Fig. 3. Distribution in $M(D^*p)$ for opposite-charge D^*p combinations, separately for $D^{*-}p$ (left) and $D^{*+}\bar{p}$ (right). Background model as in fig. 2.

$M(K\pi\pi) + M(D^*)_{PDG}$. The mass difference for the opposite-charge combinations $D^{*-}p$ and $D^{*+}\bar{p}$ is shown in fig.2. A narrow peak at $M(D^*p) \approx 3.1$ GeV is clearly visible. This signal is observed with similar strength and compatible width in the $D^{*-}p$ and $D^{*+}\bar{p}$ combinations separately (fig.3). The background under the D^*p signal can be reasonably described by the sum of two components: a non-charm background estimated from the data using the above mentioned wrong charge D combinations and a charm con-

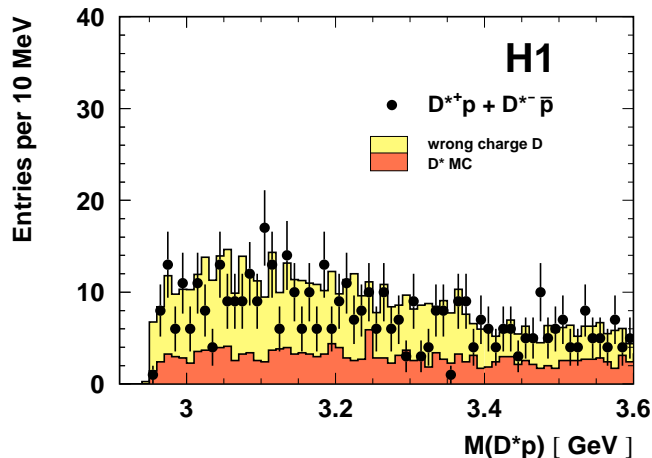


Fig. 4. Distribution in $M(D^*p)$ for same-charge D^*p combinations. Background model as in fig. 2.

tribution, where a real D^* is combined with random proton tracks. The latter is estimated from Monte Carlo simulations of the D^* production in DIS events using the RAPGAP generator [10]. No significant peak is observed in the invariant mass of the same-charge combinations, $D^{*+}p$ and $D^{*-}\bar{p}$, shown in fig.4. The data are compatible with the sum of the charm and the non-charm background.

4. Signal Tests and Significance

Extensive tests have been performed to examine the observed signal. The D^* content of the signal has been investigated by comparing the D^* signals in the signal and sideband regions of the $M(D^*p)$ distribution, using the full proton selection but no requirement on $\Delta M(D^*)$. The $\Delta M(D^*)$ distribution is shown in fig. 5 for events in a ± 15 MeV mass window around the D^*p signal, $3085 < M(D^*p) < 3115$ MeV, compared with the similar distribution from the sidebands. The $\Delta M(D^*)$ distribution from the sidebands is scaled by a factor accounting for the different widths of the sideband and signal mass windows. In the $\Delta M(D^*)$ region above the D^* peak the distributions agree with each other in shape and normalisation. However, there is a clear difference around the D^* peak position, where the distribution from the signal region in $M(D^*p)$ overshoots that from the sidebands. The signal region in $M(D^*p)$ is thus significantly richer in D^* mesons than the sideband regions.

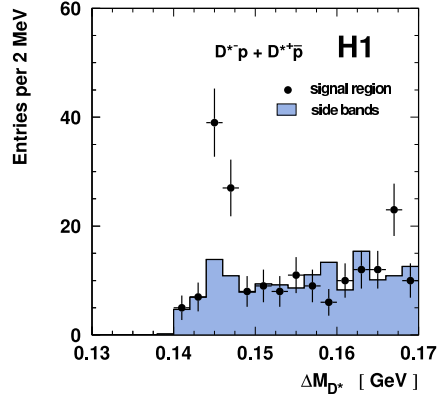


Fig. 5. $\Delta M(D^*)$ distribution for events in a 30 MeV window around the signal in the opposite-charge $M(D^*p)$ distribution, with no requirement on $\Delta M(D^*)$, compared with the corresponding distribution from the D^*p sideband regions, normalised according to the width of the mass window.

The proton content of the signal has been tested in the following way. At low proton momenta, $p(p) < 1.2$ GeV a more stringent particle identification in dE/dx can be applied. In this proton enriched sample a clear peak at $M(D^*p) \approx 3100$ MeV is visible. A harder momentum spectrum of the proton candidates in the signal region of the $M(D^*p)$ distribution compared with its sidebands was observed, as shown in fig.6. This behaviour is expected for a two-body resonance decay, since for single charged particles a steeply falling momentum distribution is expected, which is conserved when forming the combinatorial background. Whereas in case of a real resonance the decay particles can be emitted in the direction of flight of the original particle and therefore may have larger momenta in the laboratory frame. Fig.6 suggests that the signal to background ratio improves as the proton momentum increases. In fig. 7 the $M(D^*p)$ distribution is shown for momenta $p(p) > 2$ GeV without any particle identification requirement. A strong signal over a reduced background, well described by the charm and non-charm background models, is observed. The peak position and width are compatible with those observed with the standard selection.

Possible reflections from other resonances have been studied by investigating mass distributions and correlations under different mass hypothesis for the K, π and proton candidate tracks. None of these studies gave an

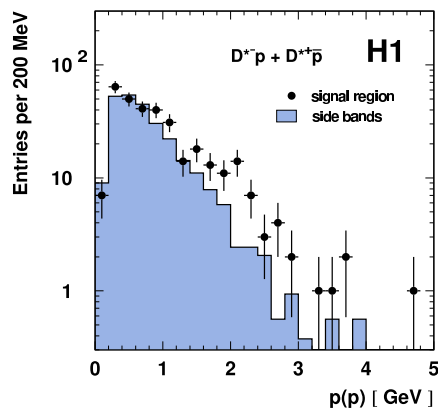


Fig. 6. Momentum distribution of all proton candidates yielding $M(D^*p)$ values falling in the signal and sideband regions of the signal in $M(D^*p)$.

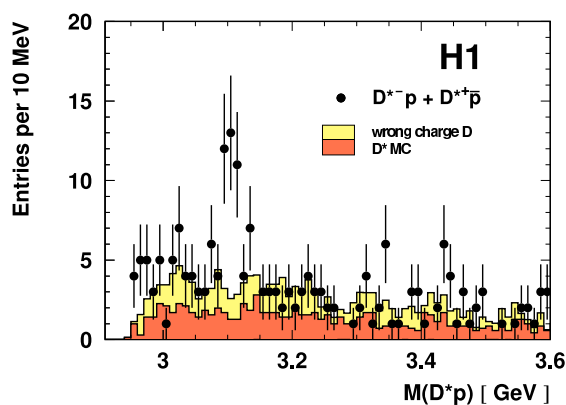


Fig. 7. $M(D^*p)$ invariant mass distribution for a high momentum selection $p(p) > 2$ GeV with no proton dE/dx requirement. The data are compared with the same background model as in fig. 2.

explanation for the observed structure. In particular the orbitally excited D_1 and D_2 states decaying to $D^*\pi$ do not give a significant contribution to the peak. An independent photoproduction sample shows a D^*p resonance structure which is compatible with the one seen in DIS events. Furthermore all events have been visually scanned without discovering any anomalies in

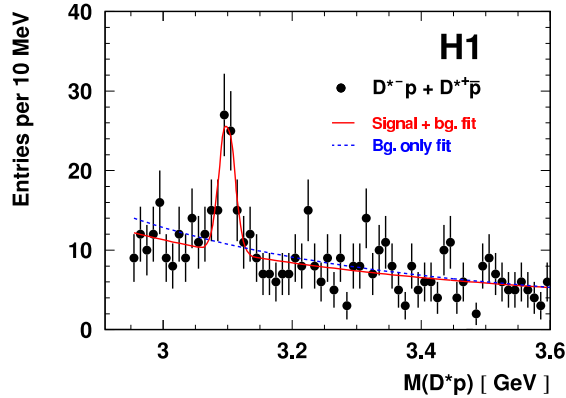


Fig. 8. $M(D^*p)$ distribution from opposite-charge D^*p combinations compared with the result of a fit including both signal and background distributions (solid line) and with a fit including only the background component (dashed line).

the reconstruction of the events neither in the signal nor in the background regions.

The signal in fig. 2 is quantified by fitting the mass distribution by a gaussian together with a background function, $\alpha[M(D^*p) - M(D^*)]^\beta$, as shown in fig. 8. The resulting peak position is $3099 \pm 3(\text{stat})$ MeV with a systematic uncertainty of 5 MeV. The gaussian width is $12 \pm 3(\text{stat})$ MeV, which is compatible with the experimental resolution of 7 ± 2 MeV. The fit yields $N_S = 50.6 \pm 11.2$ signal events under the peak, which corresponds to a raw ratio of $N_S/N(D^*)$ of $1.46 \pm 0.32\%$ of the D^* yield, not corrected for detector acceptances. In a 2σ window around the peak position $N_B = 45.0 \pm 2.8$ background events are observed. In order to estimate the significance in a more conservative approach the full distribution is fitted by the background shape without adding a gaussian to describe the signal (dashed line in fig. 8), yielding $N_B = 51.7 \pm 2.7$ background events in the above mentioned 2σ mass window. The poisson probability for an expectation of $N_B = 51.7$ events to fluctuate to the observed 95 events or more is 4×10^{-8} , which corresponds to a significance of 5.4σ in terms of gaussian standard deviations.

5. Discussion

A clear narrow resonance is observed in the invariant mass of D^*p combinations in deep-inelastic scattering events for $Q^2 > 1 \text{ GeV}^2$ with a width

compatible with the detector resolution. The signal can not be explained in terms of reflections or reconstruction failure and was robust under several tests. The background model well describes the observed background in the D^*p mass distributions. The observation of the narrow structure seen in DIS events is also observed in the analysis of an indendent photoproduction sample. However, several experiments searched for this structure and could not confirm its observation. Negative results were reported by e.g. the FOCUS, ALEPH, CDF and BELLE collaboration [11] in different reactions and different phase space regions as at H1, which complicates the direct comparison. The ZEUS collaboration [12] found no signal in the same reaction and similar kinematic cuts and phase space. The experimental discrepancy needs further investigation and clarification, possibly from the upcoming HERA-II data.

6. Conclusion

A narrow resonance is observed in $D^{*-}p$ and $D^{*+}p$ combinations at $M(D^*p) = 3099 \pm 3(\text{stat}) \pm 5(\text{syst})\text{MeV}$ with a gaussian width of $12 \pm 3(\text{stat})\text{MeV}$, compatible with the experimental resolution. The statistical significance is estimated to be 5.4σ . The observed baryonic resonance may be interpreted as anti-charmed baryon with minimal constituent quark content $uudd\bar{c}$.

REFERENCES

- [1] T. Nakano *et al.*, (LEPS), Phys. Rev. Lett. **91** (2003) 012002; S. Stepanyan *et al.*, (CLAS), Phys. Atom. Nuclei **66**, 1715 (2003); J. Barth *et al.*, (SAPHIR), Phys. Lett. B **572** (2003) 127; V. Kubarovsky *et al.*, (CLAS), Phys. Rev. Lett. **92** (2004) 03201 [erratum-ibid. 92 (2004) 049902].
- [2] V. V. Barnim *et al.*, (DIANA), Phys. Atom. Nucl. **66** (2003) 1715 [Yad. Fiz. 66 (2003) 1763]; A. E. Asratyan, A. G. Dolgolenko and M. A. Kubantsev, Phys. Atom. Nucl. **67** (2004) 682; A. Alev *et al.*, (SVD), hep-ex/0401024; A. Airapetian *et al.*, (HERMES), Phys. Lett. B **585** (2004) 127; M. Abdel-Bary *et al.*, (COSY-TOF), Phys. Lett. B **595** (2004) 127; S. Chekanov *et al.*, (ZEUS), Phys. Lett. B **591** (2004) 7.
- [3] J. Z. Bai *et al.*, (BES), Phys. Rev. D **70** (2004) 012004; BaBar Collaboration, hep-ex/0408064; BELLE Collaboration, hep-ex/0409010; S. R. Armstrong, hep-ex/0410080; S. Schael *et al.*, (ALPEH), Phys. Lett. B **599**(2004) 1; I. Abt *et al.*, (HERA-B), Phys. Rev. Lett. **93** (2003) 212003; Yu. M. Antipov *et al.*, (SPHINX), Eur. Phys. J. A **21**, 455 (2004); M. J. Longo *et al.*, (HyperCP), Phys. Rev. D **70** (2004) 111101; D. O. Litvintsev, (CDF), hep-ex/0410024; R. Mizuk *et al.*, (Belle), hep-ex/0411005; C. Pinkerton *et al.*, (PHENIX), J. Phys. G **30** (2004) 1201;

- [4] C. Alt *et al.*, (NA49), Phys. Rev. Lett. **92** (2004) 042003.
- [5] H. Lipkin, Phys. Lett. B **195** (1987) 484; C. Cignoux, B. Silvestre-Brac and J. Richard, Phys. Lett. B **193** (1987) 323; D. Riska, N. Scoccola, Phys. Lett. B **299** (1993) 338; F. Stancu, Phys. Rev. D **58** (1998) 111501; R. L. Jaffe and F. Wilzcek, Phys. Rev. Lett. **91** (2003) 232003; M. Karliner and H. J. Lipkin, hep-ph/0307343; K. Cheung, hep-ph/0308176.
- [6] A. Aktas *et al.*, (H1), Phys. Lett. B **588**(2004)17.
- [7] I. Abt *et al.*, (H1), Nucl. Inst. Meth. **A386**(1997)310; I. Abt *et al.*, (H1), Nucl. Inst. Meth. **A386**(1997)348.
- [8] Particle Data Group Collaboration, Phys. Rev. D **66** (2002) 010001.
- [9] J. Steinhart, 'Die Messung des totalen $c\bar{c}$ -Photoproduktions-Wirkungsquerschnittes durch die Rekonstruktion von Λ_C Baryonen unter Verwendung der verbesserten dE/dx Teilchenidentifikation am H1 Experiment bei HERA', Ph.D. thesis, 1999, Universität Hamburg (in german, available from http://www-h1.desy.de/publicatons/theses_list.html).
- [10] H. Jung, Comput. Phys. Commun. **86** (1995) 147; <http://www.desy.de/~jung/rapgap.html>.
- [11] S. Schael *et al.*, (ALEPH), Phys. Lett. B **599** (2004) 1; R. Mizuk (BELLE) hep-ex/0411005; J. Bei *et al.*, (BES), Phys. Rev. D **70** (2004) 012004; I. Gorelov (CDF), hep-ex/408025; K. Stenson (FOCUS), hep-ex/0412021.
- [12] S. Chekanov *et al.*, (ZEUS), Eur. Phys. J. C **38** (2004) 29.